

# **Liquid and particles retention in foamed suspensions**

Sylvain Guignot<sup>1</sup>, Sylvain Faure<sup>1</sup>, Michèle Vignes-Adler<sup>2</sup> and Olivier Pitois<sup>2\*</sup>.

<sup>1</sup> Advanced Decontamination Processes Laboratory, Commissariat à l'Energie Atomique (CEA Marcoule), CEA, DEN, SPDE, LPAD, 30207 Bagnols sur Cèze, France.

<sup>2</sup> Université Paris-Est, Laboratoire de Physique des Matériaux Divisés et des Interfaces, UMR CNRS 8108, 5 bvd Descartes, 77454 Marne la Vallée Cedex 2, France.

\* Corresponding author: Fax: +33 1 60 95 72 97

\*E-mail address: [olivier.pitois@univ-mlv.fr](mailto:olivier.pitois@univ-mlv.fr)

## **Abstract**

This article describes a new strategy to modify the drainage behaviour of aqueous foams with solid nanoparticles. While for high particulate concentrations the liquid flow can be slowed down owing to viscosity effects, we show that much less concentrated systems, but possessing peculiar physicochemical properties, can also strongly modify the drainage behaviour. Taking advantage of the agglomerated state of pyrogenic silica in aqueous media, highly porous *macro-particles* are specifically prepared in the initial foaming solutions. It is shown that their typical size and their intrinsic yield-stress properties enable them to be captured by the bubbles during the foam generation stage and subsequently to be retained in the foam channels, according to a geometrical criterion based on the particle/bubble sizes ratio. The drainage curves of the foams display significant retention rates for the suspension during several hours, an effect that is enhanced for higher particles concentrations. This has been related to the high internal porosity and hydrophilic character of the macroparticles, acting as liquid-traps in the foam microstructure.

**Keywords:** Bubble columns, foam, particulate processes, non-newtonian fluids, filtration, porous media.

## 1 INTRODUCTION

An aqueous foam can be viewed as a dispersion of gas bubbles in a liquid, stabilized by surface-active species adsorbed at the gas-liquid interfaces. The foam structure is described by the Plateau rules stating that the liquid films between the bubbles meet three by three to form Plateau borders, these latter intersecting four by four at nodes (Weaire and Hutzler, 1999). Like in solid porous materials, the liquid flows through the continuous network of interconnected channels that constitutes the main part of the *foam porosity*. Foam ages because of several interrelated physical processes, namely the liquid drainage in films and channels, the so-called disproportionation process, and the coalescence of bubbles. As a major destabilizing effect of drainage, the liquid films thin progressively, thus promoting their rupture and the resulting collapse of the foam sample. Moreover, the films thinning eases the gas diffusion from smaller to larger bubbles driven by their different internal pressures. In return, the disproportionation process enhances the liquid drainage (Saint-Jalmes, 2006). As the collapse of the foam can be detrimental to potential applications, a possible strategy to enhance the foam stability is precisely to reduce the liquid drainage. This is traditionally achieved by means of viscosifiers such as Xanthan gum (Faure et al., 2004; Safouane et al., 2006). Alternatively, the effect of disproportionation on foam drainage can be reduced by using poorly soluble gas (Saint-Jalmes, 2006). With the same purpose, new trends propose to cancel out the gas pressure differences between bubbles, by using foams with bubbles as monodisperse as possible – so called crystalline foams (Vignes-Adler and Weaire, 2008). Following the more recent findings, solid colloidal particles can be added to the formulation: mineral particles may replace the liquid-thickening organic agent, which may be of paramount interest for industrial applications. Moreover, these particles can be specifically

hydrophobized for an optimal adsorption at the liquid/gas interface, thus acting as an armor for the bubbles, preventing coalescence and reducing the internal gas transfer (Binks, 2002; Abkarian, 2007; Martinez et al., 2008). On the other hand, hydrophilic particles remain confined in the liquid phase and their ability to enhance the foam stability is less obvious. They are believed to impede global liquid flows by narrowing channels and forming local plugs in the foam, but yet, illustrative experimental data for these mechanisms remain scarce. Monodisperse colloidal particles were found to slow down the thinning of horizontal liquid films and make it occur in a stepwise manner as shown by Sethumadhavan et al. (2001). This is ascribed to an additional contribution to the disjoining pressure in the films brought by the ordering particles. However, this significant stabilizing effect is reduced as the liquid film drains vertically (Hudales and Stein, 1990; Garrett et al., 2006). On a wider scale, Kruglyakov and Taube (1972) have studied the drainage of foams generated from a non-ionic surfactant suspension of pyrogenic silica. Results showed that the loss of liquid is slightly slowed down when particles are present, and this was explained by a steric hindrance to the liquid flow. To significantly affect the drainage of a foam, the overstepping of some gelification point in the liquid phase seems to be required. Wilson (1980) thus designed very stable foams by using concentrated suspensions of micrometric polystyrene beads, and showed that this stability was due to the formation of a whole gelified network embedding particles both at the interfaces and in the liquid. This configuration could only be attained when the physicochemical conditions of particles coagulation were fulfilled in the solution. Given the high viscosities of these particular foaming suspensions, specific foam generation methods have to be carried out.

In this paper, we investigate an alternative strategy to enhance the retention of both liquid and nanoparticles in foams without resorting to concentration effects. This is achieved through the in-situ making of highly porous agglomerates, the so-called *macro-particles*, in

the foaming solution. Note that these *macro-particles* must be understood as inert objects resulting from a preliminary “conditioning” stage, which definitely distinguish the present approach from those based on reactive suspensions (Carn et al., 2009). Provided that these macro-particles have appropriate typical sizes, they are likely to be captured by the foam channels. As a necessary property, they must be strong enough to withstand the shears exerted by the liquid flowing in the foam and thus to behave as effective corks. In the following, we describe the preparation of the foaming suspensions used for testing this strategy. The size and the rheology of the resulting macroparticles is then studied. Dedicated experiments are performed to investigate the behavior of the macroparticles in foams.

## **2 MATERIALS AND METHODS**

### **2.1 Preparation of the foaming suspensions**

The surfactant used to stabilize the foams is a mixture of three well-defined alkylpolyglycosides (Glucopon 215 CS supplied by Cognis, France). Its critical micellar concentration in demineralized water is around  $0.6 \text{ g.L}^{-1}$  (determined by the surface tension dependence on the concentration). In all the experiments, it was introduced without further purification to get a base-solution at  $10 \text{ g.L}^{-1}$ . The corresponding surface tension is  $\sigma \approx 27 \text{ mN.m}^{-1}$ .

The suspensions of interest for the present study are obtained by adding various quantities of pyrogenic silica (Aerosil 380, Evonik) into equal volumes (300 mL) of the foaming base solution. Each suspension is then stirred (magnetical stirrer bar of 5.7 cm) in a beaker of 400 mL (diameter 7.5 cm), at a fixed speed (600 rpm) during 5 min, before

adjusting the pH values to 7.0 using nitric acid and a pH-meter. The resulting solution is a suspension of agglomerates. These later are known to be composed of aggregates in a loose packing arrangement (Iler, 1979), and are therefore called *macro-particles* in the following. The agglomerated state was checked by applying brief ultrasonic impulses of 50 W with an ultrasonic probe during 10 minutes in the solution. Afterwards, dynamic light scattering was performed on a sample of this suspension and showed a size distribution ranging from 140 nm to 620 nm centered on  $\sim 290$  nm. This size indeed corresponds to the expected aggregates, resulting from the irreversible sintering of the primary silica units (the size is 7 nm, the BET specific surface is  $380 \pm 30 \text{ m}^2.\text{g}^{-1}$ , and the density is  $\rho_{\text{SiO}_2} = 2200 \text{ kg.m}^{-3}$ ). Eisenlauer and Killmann (1980) have determined the mean porosity of this type of colloidal clusters to be around 0.9, meaning that they enclose high amounts of the dispersion fluid. Note that the results presented in the following are obtained from the *macro-particles* suspensions, i.e. not sonicated solutions.

## 2.2 Characterization of the foaming suspensions

### 2.2.1 Size of the macro-particles

The size of the resulting *macro-particles* are obtained from settling measurements (Font et al., 1994). Each suspension at concentration  $C_s$  is homogenized in a test tube. The initial height of suspension is  $H_0$ . The evolution of the height  $H$  corresponding to the clarification front is then followed using a CCD camera, allowing for the settling rate  $-dH/dt$  to be measured. Assuming that the *macro-particles* are equally-sized, sphere-shaped, and

impermeable, their apparent diameter,  $d_m$ , is deduced from the relation proposed by Snabre and Mills (2000) for monodisperse rigid spheres:

$$d_m^2 = -\frac{18\mu}{(\rho_m - \rho)g} \frac{dH/dt}{\phi} \left[ 1 + 5.8 \frac{1-\phi}{\phi} \right], \quad (1)$$

where  $g$  is the gravitational acceleration,  $\mu$  and  $\rho$  are respectively the dynamic shear viscosity and the density of the suspending liquid,  $\rho_m$  is the density of the *macro-particles* and  $\phi$  is the *macro-particles* volume fraction in the suspension. The two later parameters are determined from the experiment. Indeed,  $H$  is found to decrease until a constant value,  $H_f$ , is reached.  $H_f$  corresponds to the packing of the *macro-particles* at the bottom of the tube. The packing fraction is expected to be  $\phi_{pack} \approx 0.5$ . Note that  $H_f$  is measured over the time scale of the primary settling, i.e. 1-10 minutes. Over larger time scales, i.e. hours and days, a subsequent slow decrease is observed, meaning that the packing fraction and presumably the SiO<sub>2</sub> concentration in the *macro-particles*,  $C_m$ , increase. As the kinetic of this subsequent evolution is several orders of magnitude smaller than the first one, it is disregarded in the following.  $\phi$  is thus given by  $\phi = \phi_{pack} H_f / H_0$ , and the *macro-particles* density is:

$$\rho_m = \rho + C_m (1 - \rho / \rho_{SiO_2}), \text{ where } C_m = C_s / \phi.$$

### 2.2.2 Rheology of the *macro-particles*

The rheological properties of the suspensions are measured with a controlled stress rheometer Bohlin C-VOR equipped with concentric cylinders (inner space: 1.25 mm). The temperature is set around  $26.0 \pm 0.02$  °C. Successive constant stresses (ranging from 0.005 Pa

to 6 Pa) are applied during 30 s, and the resulting deformations are measured. A pre-shearing at  $50 \text{ s}^{-1}$  during 10 s, followed by a resting time of 30 s, is applied prior to each stress step. The surface of the two cylinders is notched to prevent any wall slip. Studied concentrations range from 40 to  $90 \text{ kg.m}^{-3}$  of introduced silica. Only suspensions with a concentration above  $40 \text{ kg.m}^{-3}$  are considered, since for lower concentrations the gravity settling process results in a phase separation that disturbs the rheological measurements.

## 2.3 Foam experiments

### 2.3.1 Retention and release of macro-particles in foams

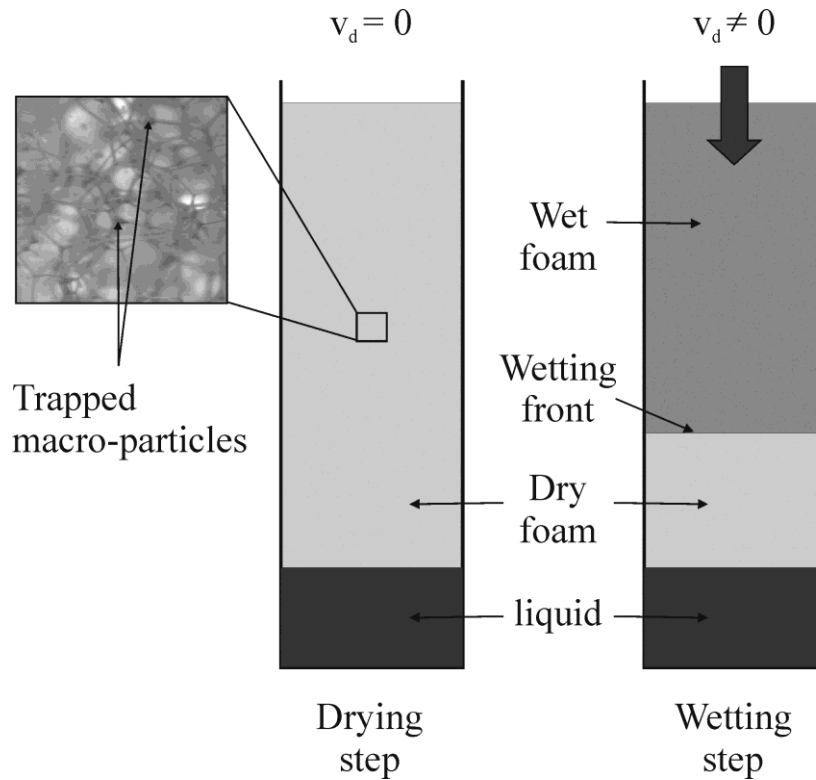


**FIG 1.** Diagram of the experiment dedicated to the *macro-particles* trapping in aqueous foams. Wetting and drying steps are successively performed. During wetting steps, particle free solution is introduced in the foam column at a given flow rate, so that the liquid fraction



is suddenly increased in the foam. Each wetting step is followed by a drying step to observe the *macro-particles* in the foam (see the photo). The liquid flow rate of wetting steps is gradually increased, and the liquid fraction for which the *macro-particles* are expelled out of the foam is measured for several foams with different bubble size.

Foams are generated by a gentle bubbling of perfluorohexane-saturated nitrogen in the silica-free foaming solution by means of a syringe needle, until  $\sim 25$  cm-high foams are made. Perfluorohexane is used to limit the gas diffusion during the experiment, and thus to keep an almost constant bubble size. The foam is let draining until it becomes dry, and a few milliliters of the *macro-particles* suspension is introduced in the foam by a microsyringe equipped with a thin rubber tubing. The small amount of suspension is deposited in the central part of the foam, in order to avoid disruptive top and bottom end effects, i.e. collapse of bubbles at the top and capillary rising from the tank of foaming suspension upon which the foam lies. In the dry state of the foam, *macro-particles* can be distinguished in the foam liquid network (as the liquid fraction increases they cannot be observed anymore). From this state, a wetting step is performed: the upper part the foam is wetted by given flow rate of particle free foaming solution. This wetting step allows for the liquid fraction to be precisely measured: a resulting steadily-moving liquid front progresses downwards in the dry foam at a velocity  $v_f$  (Weaire et al., 1997), accompanied with a dilatation of the foam channels. The liquid front velocity  $v_f$  is related to the superficial velocity of the injected liquid,  $v_d$ , by  $v_d/v_f = \varepsilon$ , where  $\varepsilon$  is the foam liquid fraction (see Fig. 1). After the passage of the wetting front, the liquid fraction is uniform over the whole foam sample: its value depends on  $v_d$ . Each wetting step is followed by a drying step to observe the *macro-particles* in the foam (see the photo in Fig. 1). The liquid flow rate of wetting steps is gradually increased, and the liquid fraction for

which the *macro-particles* are expelled out of the foam is measured for several foams with different bubble size. Note also that we observe the foam/liquid area at the bottom of the column to check that *macro-particles* are definitely expelled out of the foam.

### 2.3.2 Free drainage experiment of foams

The measurements have been performed with a commercially available device, Foamscan (Teclis, France). Compressed air at a controlled flow rate of  $100 \text{ mL.min}^{-1}$  is sparged into  $V_0 = 25 \text{ mL}$  of the foaming suspension through a removable sintered porous glass (porosity value of 3,  $16\text{-}40 \text{ }\mu\text{m}$  range) in a square rectangular column (cross-section  $S = 6.25 \text{ cm}^2$ ) fixed above. The generation is stopped when the foam has reached a definite height  $H_{foam}$  ranging between 20 and 25 cm. This height slightly decreases during the experiment, about 1 cm over 3000 seconds for the foam generated from the less concentrated suspension. This decrease is taken into account in the calculation of the liquid fraction. The liquid fraction is known at  $\pm 0.01$ .

The bubbles sizes in the foam are polydisperse and the sparging is adjusted so that the initial liquid fraction,  $\bar{\varepsilon}_0$ , is close to  $0.1 \pm 0.01$ . A couple of vertical electrodes fixed at the bottom of the column performs a conductivity measurement every second. The contribution of the foam phase to the obtained signal is negligible so that the conductivity value accounts for the height and thus the volume  $V$ , of liquid remaining at the bottom of the column. The precise relation between conductivity value and  $V$  requires a calibration step. This has been made before the experiment on the foaming suspension. The mean liquid fraction in the foam is thus determined as:  $\bar{\varepsilon} = (V_0 - V) / SH_{foam}$ . During the experiments, pictures of the bubbles touching

one of the inner transparent walls of the squared-column are taken, and an image processing software is used to extract the size distribution of the bubbles.

### 3 RESULTS

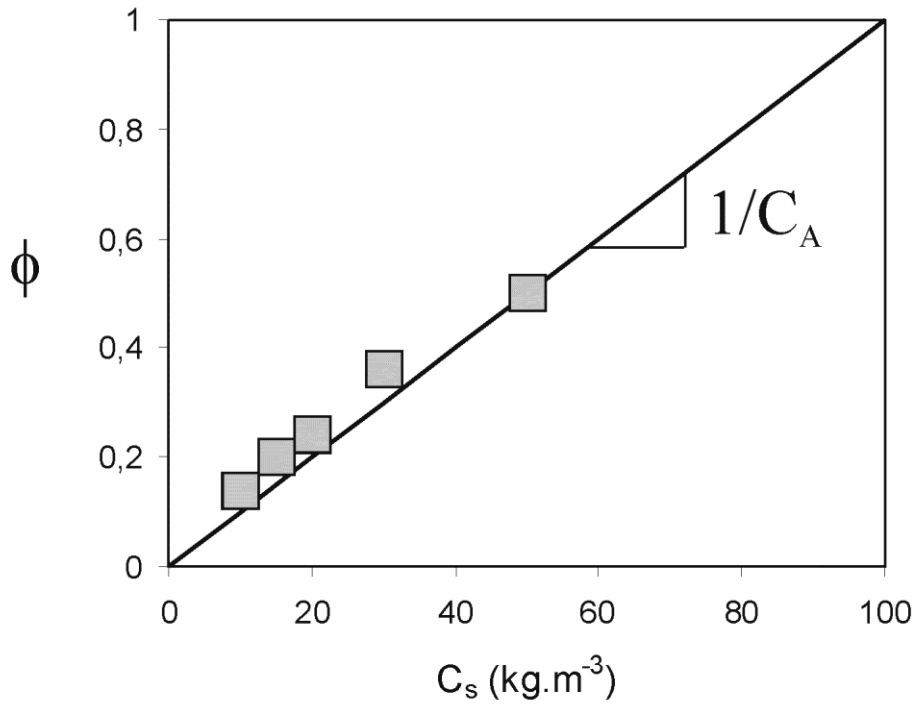


**FIG 2.** Volume fraction filled by silica agglomerates in the suspension as a function of the particles concentration.

The volume fraction of the *macro-particles* in the suspension,  $\phi$ , is a linear function of the particles concentration  $C_s$  (Fig. 2). The slope  $p$  is related to the particles concentration in the agglomerates:  $p = 1/C_m \approx 10^{-2} \text{ m}^3.\text{kg}^{-1}$ . For concentration values equal or above  $50 \text{ kg.m}^{-3}$ , the sedimentation is small or even negligible over several minutes, meaning that the packing fraction is obtained for  $C_s \approx 50 \text{ kg.m}^{-3}$ . The internal porosity of the agglomerates,  $\psi_m$ , can be

calculated with:  $\psi_m = 1 - C_m / \phi_{pack} \cdot \rho_{SiO_2}$ . With  $C_m = 100 \text{ kg.m}^{-3}$ , we find  $\psi_m \approx 0.95$ , meaning that the *macro-particles* are very loose and essentially composed of foaming solution. The size of the *macro-particles* is calculated from the settling velocity, the volume fraction and the density of the *macro-particles*. For the investigated suspensions, we obtain  $70 \text{ }\mu\text{m} < d_m < 90 \text{ }\mu\text{m}$ . Additionally, the maximum error bar on the *macro-particles* diameter is estimated to be  $15 \text{ }\mu\text{m}$ .

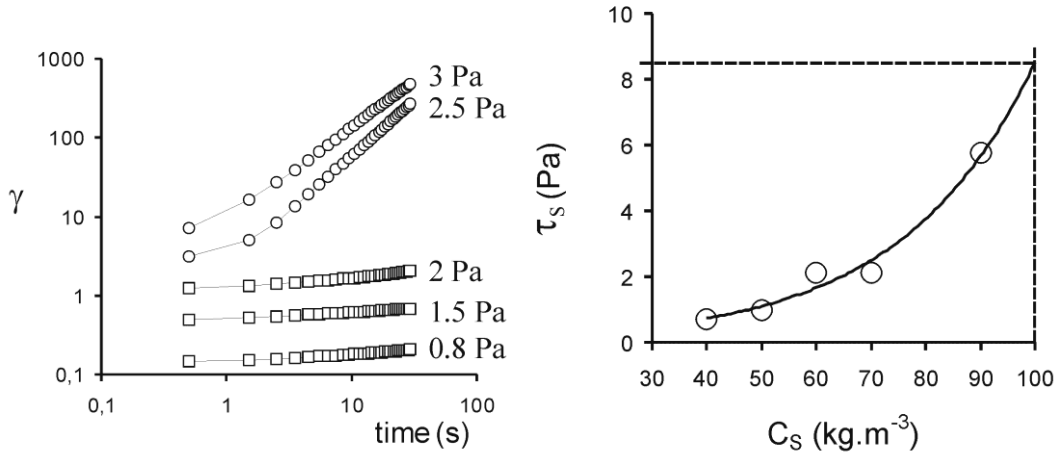


**FIG 3.** (a) Deformation of a suspension containing  $60 \text{ kg.m}^{-3}$  Aerosil 380 in a Glucopon 215 mixture at pH 7, as a function of time, for various applied stress levels. (b) Measured yield stresses as a function of Aerosil concentration (pH 7)

Fig. 3a shows the creep flow measurements obtained for a suspension at  $60 \text{ kg. m}^{-3}$  submitted to various stresses ranging from 0.8 to 3 Pa. For the lower applied stresses (below 2 Pa) the deformation remains almost constant during the measurement, while it abruptly increases for greater stress levels and reaches values several orders of magnitude higher than at 2 Pa. This suspension behaviour thus evolves from an elastic solid to a viscous liquid as the stress is raised. The transition value corresponds to a yield stress,  $\tau_s$ , and can be estimated in

this specific case to be between 2 and 2.5 Pa. This behavior has been found for all the studied samples. Fig.3b reports the obtained yield-stress values for suspensions with various silica concentrations. The observed rise is ascribed to the denser entanglement of the *macro-particles* due to the increase in their effective volume fraction in the suspension. We were not able to prepare suspensions at  $C_s = C_m$ , i.e.  $100 \text{ kg.m}^{-3}$ , with the current method. However, the corresponding value can be reasonably extrapolated from the data:  $\tau_s(C_s = C_m) \approx 8\text{-}10 \text{ Pa}$ .

Finally, note that the thixotropic character of the suspensions was observed during the rheology measurements. The displayed yield stress value is therefore closely related to the ratio between the duration of the stress application and a characteristic time of relaxation in the suspension (Deborah number). It means that over large durations, the solid/liquid transition can be observed as a function of time if the applied stress is slightly below the reported yield stress.

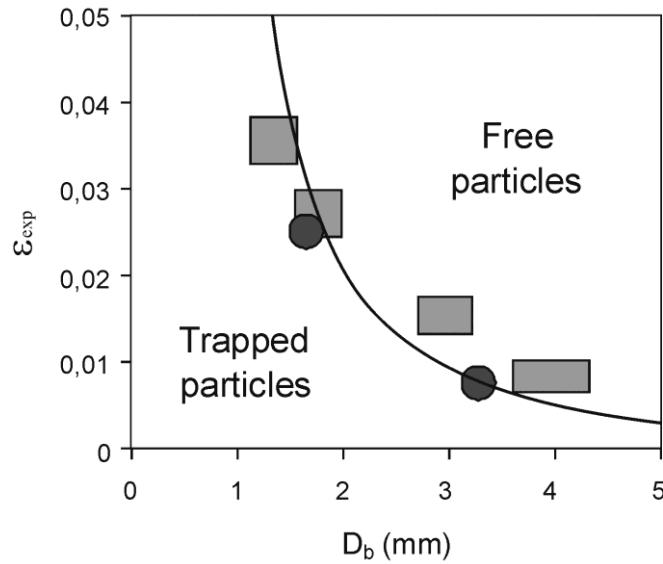


**FIG 4.** Critical liquid fraction corresponding to the release of trapped particles in the foam, as a function of the foam bubbles mean diameter. Rectangles correspond to silica agglomerates (with diameter  $80 \mu\text{m}$ ), circles correspond to polystyrene beads with the same diameter, the solid line corresponds to eq.(3).

Results for the release/retention experiment are presented in the following. It turns out that the *macro-particles* are expelled from the foam above well-defined values for the liquid fraction. This value, which is referred in the following to as the critical liquid fraction  $\varepsilon_{exp}$ , depends on the bubble diameter.  $\varepsilon_{exp}$  is plotted as a function of the bubble diameter in Fig.4. Foams with small bubbles require larger liquid fractions than foams with large bubbles to expel the *macro-particles* : from almost 4 % for  $D_b \approx 1.3 \mu\text{m}$  to 1 % for  $D_b \approx 4 \text{ mm}$ . Visual observations during the experiments reveal that the *macro-particles* deform, jam in the foam or are convected by the suspending liquid between the bubble if the gaps are sufficiently large, but they do not flow as a liquid through the foam.

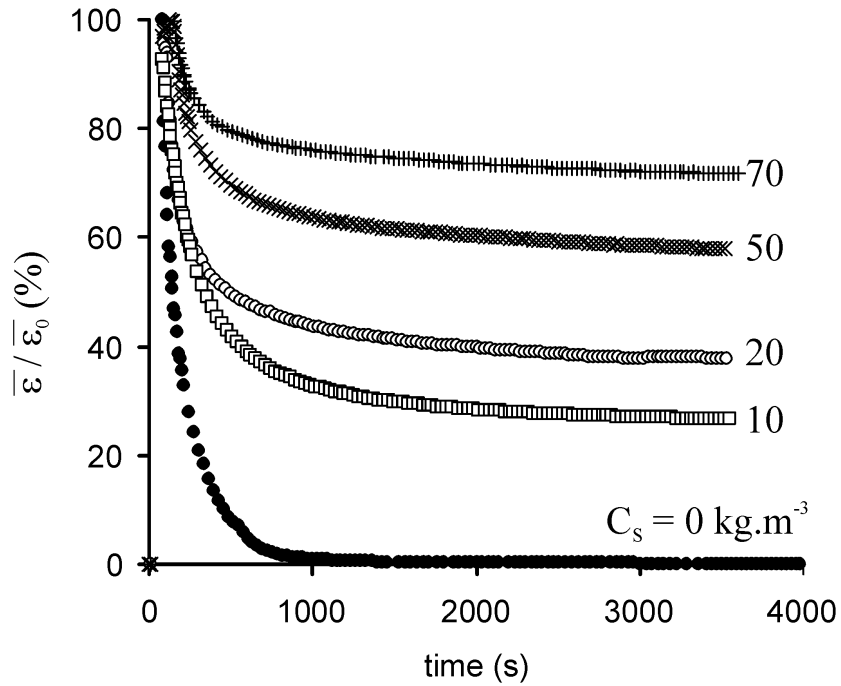


**FIG 5.** Time evolution for the mean liquid fraction in a free-drainage configuration for foams containing silica particles at a concentration  $C_s = 0$  (no particles), 10, 20, 50, 70  $\text{kg.m}^{-3}$ . The image only illustrates the retention mechanism for the particulate suspension in the foam (note that it has been obtained with other experimental conditions)

Fig.5 represents the evolution with time of the mean liquid fraction  $\bar{\varepsilon}$  of foams with various particles contents in the free drainage configuration, for which the liquid fraction varies with both space and time. The values are normalized by  $\bar{\varepsilon}_0 = 0.1 \pm 0.01$ . The results corresponding to the particle free solution are taken as the reference, to which foamed particulate suspensions will be compared. After a short hold-up time (Exerowa and Kruglyakov, 1998), the curve exhibits a strong decrease in the mean liquid fraction during the first hundred seconds and rapidly reach a ratio  $\bar{\varepsilon}/\bar{\varepsilon}_0$  of the order of a few percents. Then, the kinetics is strongly reduced and the liquid fraction slowly evolves towards the static equilibrium value. In spite of the high concentration in surfactant, the foam slowly collapses over such large time scales that the static equilibrium is never reached. Results obtained for the particulate suspensions strongly contrast with the reference behaviour. For all investigated suspensions, the first regime of rapid drainage is observed. In fact, the kinetics is not drastically affected by the presence of the *macro-particles*, which suggests that the effective viscosity of the draining phase remains close to that of the suspending liquid. However, the duration of this first regime seems to be all the shorter as the particle concentration is high. More surprisingly, the values for the static equilibrium seem to be shifted towards higher liquid fractions. In other words, significant liquid retentions appear in particulate foams, and persist for at least several hours. Measured bubble diameters were found to differ for all investigated samples. However, all average diameters spread within the range 50-100  $\mu\text{m}$  with a mean standard deviation approximately equal to 25  $\mu\text{m}$ . These deviations in the values of the bubble size cannot be responsible for the spectacular effects observed in the drainage behaviour as the particulate concentration is varied.

## 4 DISCUSSION

Results presented in the previous section indicate that whereas highly concentrated suspensions are wholly gelified, at low concentrations, the preparation method makes separate agglomerates, the so-called *macro-particles*. Within the range  $10 \text{ kg.m}^{-3} \leq C_s \leq 50 \text{ kg.m}^{-3}$ , the silica concentration in the *macro-particles* is found to be approximately constant and equal to  $C_m \approx 100 \text{ kg.m}^{-3}$ , corresponding to highly porous structures containing 95% of liquid. As a result, the volume fraction filled by the *macro-particles* in the solution is given by  $\phi = C_s / C_m$ , and the concentration  $C_s = 50 \text{ kg.m}^{-3}$  approximately corresponds to the loose packing of the *macro-particles* in the solution. The size of the resulting *macro-particles* is about  $80 \text{ }\mu\text{m}$  in diameter. Rheological tests indicate that the behaviour of the *macro-particles* is *solid-like* for weak applied stresses (a few Pascals). However, a flow behaviour is observed as the yield stress is exceeded. In the following, we consider the silica solutions as suspensions of spherical *macro-particles* at a volume fraction  $\phi = C_s / C_m$ , with diameter  $d_m$ , porosity  $\psi_m$  and yield stress  $\tau_s (C_s = C_m)$ .

Experiments performed in the foam show that for a given bubble size, trapped *macro-particles* are expelled from the foam above a given liquid fraction  $\varepsilon_{\text{exp}}$ . Since the *macro-particles* must pass through a series of Plateau borders to move in the foam, we propose to rationalize the results of Fig. 4 by introducing the parameter  $\lambda$ , which compares the size of the *macro-particles* with the characteristic size of the Plateau borders opening:  $\lambda = d_m / d_{pb}$ .  $d_{pb}$  is the diameter of the circle inscribed in the cross-section of a Plateau border in the foam. Using  $r$ , the radius of curvature defining the Plateau border cross-section, the Plateau borders



opening writes  $d_{pb} = 2\left(2/\sqrt{3}-1\right)r$ . For dry foams, a simple relation can be used to relate  $r$  to the bubble diameter and to the foam liquid fraction:  $r \propto \delta D_b \varepsilon^{1/2}$ , where  $\delta \approx 0.87$  is a constant (Weaire et al., 1997). The parameter  $\lambda$  can be expressed as:

$$\lambda = \frac{d_m}{d_{pb}} = C \frac{d_m}{D_b} \varepsilon^{-1/2} \quad (2)$$

with  $C^{-1} = 2\delta\left(2/\sqrt{3}-1\right) \approx 3.8$ . A purely geometrical criterion describing the transition between the trapped state and the free state for the macroparticles in the foam therefore writes  $\lambda = 1$ . Taking into account equation (2), the criterion becomes:

$$\varepsilon_{\text{exp}} = C^2 \frac{d_m^2}{D_b^2} \quad (3)$$

The solid line in Fig. 4 shows eq.(3). The experimental data appear to be reasonably described by the criterion, meaning that the macroparticles are expelled as soon as their mean diameter is equal to that of the Plateau borders cross-section. Additional measurements have been performed with solid polystyrene beads of well-defined diameters (80  $\mu\text{m}$ ). As illustrated in Fig. 4, the particles expulsion is also well described by eq.(3). Two conclusions can then be drawn. Firstly, the transition between the trapped state and the free state for solid particles in the foam can be reasonably described with the geometrical criterion given by eq. (3). Secondly, the intrinsic rheological properties of the *macro-particles*, i.e. thixotropy and yield stress behaviour, do not induce a drastic effect on this transition.

Results presented in Fig. 5 can now be analysed. At the early stage of drainage, values for  $\lambda$  can be obtained from the median diameter of the bubble size distribution. Whatever the sample, we obtain  $\lambda > 10$ . Note however that eq.(2) does not stand for wet foams. On the other hand, in the random packing limit for the bubbles,  $d_{pb} = (2/\sqrt{3} - 1)D_b$ , and the criterion  $\lambda = 1$  corresponds to  $d_m/D_b = 0.154$ . The macroparticles are thus definitely trapped in the foams and are then squeezed between the bubbles. The stress experienced by the *macro-particles* can be assessed from the osmotic pressure of the foam

$\Pi = 14.6\sigma(0.26 - \varepsilon)^2 / D_b \varepsilon^{1/2}$  (Höhler et al. 2008). With  $D_b \sim 10^{-4}\text{m}$ ,  $\Pi \sim 8 \text{ Pa}$  for  $\varepsilon = 0.2$ ,  $\Pi \sim 200 \text{ Pa}$  for  $\varepsilon = 0.1$ , and  $\Pi \sim 600 \text{ Pa}$  for  $\varepsilon = 0.05$ . Thus, the yield stress of the *macro-particles* is not sufficient to counteract the pressure exerted by the bubbles. The *macro-particles* deform and their shape evolves to fit the foam porosity. But why do they not flow as a liquid out of the foam with the suspending liquid? One can firstly consider the mechanical equilibrium of a yield stress fluid in the confined geometry under gravity, which can be written:

$\tau_s/r \square \rho g$  (Chaplain et al., 1992). For a foam with  $D_b \sim 100 \mu\text{m}$  and  $\varepsilon = 0.05$ ,  $r \approx 20 \mu\text{m}$  and  $\tau_s/r \approx 50 \cdot 10^4 \text{ Pa}\cdot\text{m}^{-1}$ . This means that as the foam porosity is filled with *macro-particles*, their yield stress is likely to oppose the driving force, which would result in the clogging of the foam and the retention of the suspending liquid contained within the porosity. This scenario would certainly take place in a solid porous material, but for foams, one has to take into account the fluid nature of the confining “walls”. Indeed, it is highly conceivable that the high interfacial mobility (Dame et al., 2005) promotes the flow of the suspending liquid around the confined *macro-particles*. In other words, the suspending liquid easily percolates through the obstructed porosity. In contrast to its solid counterpart, the porosity of the aqueous foams cannot be clogged, which enables the suspending liquid to drain out of the foam in spite of the geometrical obstruction of the liquid network. As a result, the final liquid fraction in the foam

corresponds to the liquid contained within the trapped, porous *macro-particles*. Assuming that the *macro-particles*' porosity remains constant and equal to  $\psi_m \approx 1$ , one can estimate that:

$$\bar{\varepsilon}_f = \phi \bar{\varepsilon}_0 + \bar{\varepsilon}_{f(C_S=0)} = \frac{C_S}{C_m} \bar{\varepsilon}_0 + \bar{\varepsilon}_{f(C_S=0)} \quad (4)$$

In the latter relation,  $\bar{\varepsilon}_{f(C_S=0)}$  is the final liquid fraction of the foam without particles.  $\bar{\varepsilon}_{f(C_S=0)}$  can be estimated from the corresponding curve in Fig. 4:  $\bar{\varepsilon}_{f(C_S=0)}/\bar{\varepsilon}_0 \approx 0.1\%$ . This value partially reflects the collapse of the foam due to the moderate stabilizing properties of the solution. This value can also be estimated from the theoretical profile for the liquid fraction as function of the foam height,  $z$ :  $\varepsilon(z)^{-1/2} = \varepsilon(z=0)^{-1/2} + zD_b(t_f)/l^2$ , with  $l = (\sigma/\rho g)^{1/2}$ ,  $\varepsilon(z=0) \approx 0.36$  and  $D_b(t_f) \approx 2 \cdot 10^{-3}$  m is the bubble diameter at the end of the experiment.

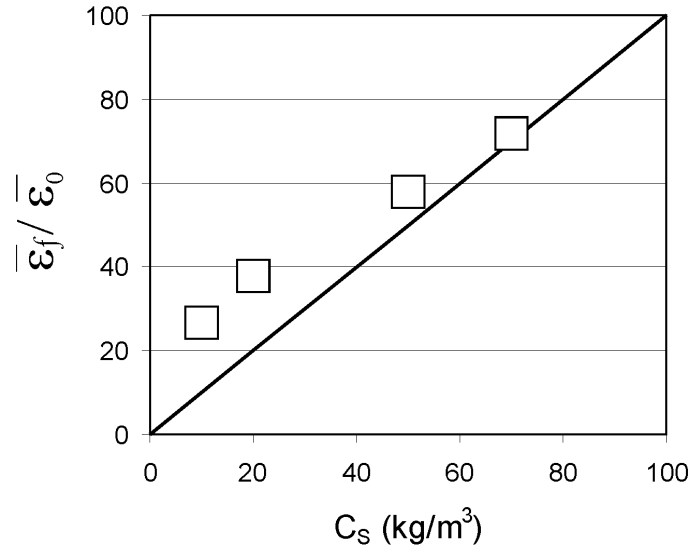


**FIG 6.** Variation of the liquid fraction retained in the foam with the initial particle concentration.

The average liquid fraction in the foam is thus  $\bar{\varepsilon} = (1/H_{foam}) \int_0^{H_{foam}} \varepsilon(z) dz \approx 10^{-3}$ . This value is consistent with the present experimental result and suggests to neglect  $\bar{\varepsilon}_{f(C_s=0)}$  in the following. Fig. 6 presents the experimental values for the ratio  $\bar{\varepsilon}_f / \bar{\varepsilon}_0$  as a function of the silica concentration. Eq.(4) is plotted for comparison, showing a good qualitative agreement. It is however observed that the theoretical prediction underestimates the final liquid fraction at the lower particles concentrations. It is believed that macroparticles are preferentially trapped during the early stage of the foam generation, inducing an increase of the effective macroparticles volume fraction,  $\phi_{eff}$ , with respect to the initial volume fraction in the solution:  $\phi_{eff} > \phi$ . This effect is expected to be more pronounced for dilute suspensions and ceases as  $\phi$  approaches the packing value. The volume of suspension initially held up by the bubbles is half of the total suspension volume introduced into the foaming column, meaning that potentially  $\phi_{eff} = 2\phi$ . Therefore, the apparent disagreement observed at low concentration should be attributed to the foam generation process rather than to the drainage properties of the resulting foam. At higher concentrations, a very good quantitative agreement is found, which substantiates the proposed liquid retention mechanism. Such a reported mechanism is expected as soon as yield stress materials are introduced into the foam ‘porosity’. To this regard, the previously observed draining behavior of foams containing oil droplets (Koczo et al., 1992) could be understood with elements proposed in the present paper: during a first stage, the suspending liquid drains faster than suspended droplets, so that the droplets volume fraction increases in the foam porosity (up to 80%), and then stop. We believe that the observed stop of drainage results from the significant intrinsic yield stress property of emulsions.

## 5 CONCLUSION

We have studied the drainage behaviour of aqueous foams made by air sparging through foaming particulate suspensions of pyrogenic silica. We have proven that a spectacular enhancement of both the liquid and particle retentions in foam could be achieved provided that a new strategy is carried out. Taking advantage of the agglomerate state of pyrogenic silica in aqueous media, highly porous *macro-particles* have been specifically prepared in the initial foaming solutions. It was then shown that their typical size and their intrinsic yield-stress properties enable them to be captured by the bubbles during the foam generation stage and subsequently to be retained in the foam channels. As an additional advantage of this method, the retention efficiency is observed from the lowest particulate concentration in the foaming suspension. The retention mechanism has been shown to be well described by a geometrical criterion relating the macro-particle and the bubbles sizes. We claim that the interesting retention mechanism is general to all types of suspensions and we thus expect the present result is useful for other systems. Finally, the drainage kinetics indicate that the suspending liquid easily percolates through the foam in spite of the geometrical obstruction imposed by the macroparticles. This behaviour suggests that, contrary to their solid counterparts, aqueous foams cannot be clogged. Further studies should investigate this striking phenomenon.

List of symbols:

- $\sigma$  surface tension of the foaming suspension
- $\mu$  bulk shear viscosity of the suspending liquid in the foaming suspension
- $\rho$  density of the suspending liquid in the foaming suspension

$\rho_{SiO_2}$	density of pure silica
$\rho_m$	density of silica <i>macro-particles</i>
$C_s$	silica concentration in the foaming suspension
$C_m$	silica concentration in the <i>macro-particles</i>
$\phi$	volume fraction of <i>macro-particles</i> in the foaming suspension
$\phi_{pack}$	packing volume fraction of <i>macro-particles</i> in the foaming suspension
$\psi_m$	porosity of silica <i>macro-particles</i>
$d_m$	diameter of silica <i>macro-particles</i>
$\tau_s (C_s = C_m)$	yield stress of silica <i>macro-particles</i>
$H_{foam}$	height of foam in the foaming column during free drainage experiments
$V_0, V$	initial and current volumes of foaming solution remaining at the bottom of the column during free drainage experiments
$\varepsilon$	foam liquid fraction
$\bar{\varepsilon}$	mean liquid fraction of foams in the foaming column
$\bar{\varepsilon}_0$	initial liquid fraction of foams in the foaming column
$\bar{\varepsilon}_f$	final liquid fraction of foams in the foaming column
$\bar{\varepsilon}_{f(C_s=0)}$	final liquid fraction of foams without silica particles
$\varepsilon_{exp}$	liquid fraction above which <i>macro-particles</i> are expelled out of the foam
$D_b$	mean diameter of foam bubbles
$r$	radius of curvature of Plateau borders (foam channels)
$d_{pb}$	diameter of passage in the Plateau borders (foam channels)
$\lambda = d_m/d_{pb}$	size ratio of <i>macro-particle</i> with the diameter of passage in the Plateau borders

## **Acknowledgements**

We gratefully acknowledge financial support from Agence Nationale de la Recherche (ANR-05-JCJC-0234-01) , from E.S.A. (MAP No. A099-108: C14914/02/NL/SH) and from the French Space Agency (convention CNES/70980).

## **References**

- Abkarian, M., Subramaniam, A.B., Kim, S.H., Larsen, R.J., Yang, S.M., Stone, H.A., 2007. Dissolution Arrest and Stability of Particle-Covered Bubbles. *Phys. Rev. Lett.* 99, 188301.
- Binks, B.P., 2002. Particles as surfactants – similarities and differences. *Current Opinion in Colloid and Interface Science.* 7, 21-41.
- Carn, F., Colin, A., Pitois, O., Vignes-Adler, M., Backov, R., 2009. Foam Drainage in the Presence of Nanoparticle-Surfactant Mixtures. *Langmuir* DOI:10.1021/la900414q
- Martinez, A.C., Rio, E., Delon, G., Saint-Jalmes, A., Langevin, D., Binks, B.P., 2008. On the origin of the remarkable stability of aqueous foams stabilised by nanoparticles: link with microscopic surface properties. *Soft Matter.* 4, 1531 – 1535.
- Chaplain, V., Mills, P., Guiffant, G., Cesari, P., 1992. Model for the flow of a yield fluid through a porous medium. *J. Phys. II.* 2, 2145-2158.
- Dame, C., Fritz, C., Pitois, O., Faure, S., 2005. Relations between physicochemical properties and instability of decontamination foams. *Colloids and Surfaces A: Physicochemical and Engineering Aspects.* 263, 210-218.
- Eisenlauer, J., Killmann, E., 1980. Stability of colloidal silica (aerosil) hydrosols. I. Preparation and characterization of silica (aerosil) hydrosols. *J. Colloid Interface Sci.* 74, 108 – 119.

Exerowa, D., Kruglyakov, P., 1998. Foam and foam films – theory, experiment, applications. Elsevier Press.

Faure S., Fournel B., Fuentes P., 2004. Composition, foam, and method for surface decontamination. *World patent WO2004/008463*.

Font, R., Marcilla, A., Colom, M.C., 1994. Aggregates of particles in dilute suspensions: estimation of aggregate volume index and diameter. *Powder Technol.* 81, 169 – 175.

Garrett, P. R., Wicks, S. P., Fowles, E., 2006. The effect of high volume fractions of latex particles on foaming and antifoam action in surfactant solutions. *Colloids and Surfaces A: Physicochemical and Engineering Aspects*. 282–283, 307–328

Höhler, R., Sang, Y.Y.C., Lorenceau, E. and Cohen-Addad, S., 2008. Osmotic Pressure and Structures of Monodisperse Ordered Foam. *Langmuir*. 24, 418-425.

Hudales, J.B.M., Stein, H.N., 1990. The influence of solid particles on foam and film drainage. *J. Colloid Interface Sci.* 140, 307-313.

Iler, R.K., 1979. The chemistry of silica. Wiley, New-York

Koczo, K., Lobo, L. A., Wasan, D. T., 1992. Effect of oil on foam stability: aqueous foams stabilized by emulsions. *J. Colloid Interface Sci.*, 150, 492-506.

Kruglyakov, P.M., Taube, P.R., 1972. Syneresis and stability of foams containing a solid phase. *Coll J.-USSR* 34 (2), 194.

Safouane, M., Saint-Jalmes, A., Bergeron, V., Langevin, D., 2006. Viscosity effects in foam drainage: Newtonian and non-newtonian foaming fluids. *Eur. Phys. J. E.* 19, 195 – 202.

Saint-Jalmes, A., 2006. Physical chemistry in foam drainage and coarsening. *Soft Matter*. 2, 836-849.



- Sethumadhavan, G.N., Nikolov, A.D., Wasan, D.T., 2001. Stability of liquid films containing monodisperse colloidal particles. *J. Colloid Interface Sci.*, 240, 105-112.
- Snabre, P., Mills, P., 2000. Settling and fluidization of non Brownian hard spheres in a viscous liquid. *Eur. Phys. J. E.* 1, 105 – 114.
- Vignes-Adler, M., Weaire, D., 2008. New foams : fresh challenges and opportunities. *Current Opinion in Colloid and Interface Science.* 13, 141 – 149.
- Weaire, D., Hutzler, S., Verbist, G., Peters, E., 1997. A review of foam drainage. *Adv. Chem. Phys.* 102, 315 – 374.
- Weaire, D., Hutzler S., 1999. The physics of foams. *Oxford University Press, Oxford.*
- Wilson, J.C., 1980. A study of particulate foams. *Doctoral dissertation*, University of Bristol.